Supramolecular Materials: Molecular Packing of Tetranitrotetrapropoxycalix[4]arene in Highly Stable Films with Second-Order Nonlinear Optical Properties

Paul J. A. Kenis, Oscar F. J. Noordman, Holger Schönherr, Esther G. Kerver, Bianca H. M. Snellink-Ruël, Gerrit J. van Hummel, Sybolt Harkema, Cornelis P. J. M. van der Vorst, Jeff Hare, Stephen J. Picken, Johan F. J. Engbersen, Niek F. van Hulst, G. Julius Vancso, and David N. Reinhoudt*

Abstract: Highly stable films of tetranitrotetrapropoxycalix[4]arene (**9**) with second-order nonlinear optical (NLO) properties and a noncentrosymmetric structure were obtained by a novel crystallization process at 130–140 °C in a dc electric field. The packing of **9** in these films was elucidated by a combination of X-ray diffraction, angle-dependent second-harmonic generation, and scanning force microscopy (SFM). The experimental results agree well with solid-state molecular dynamics calculations for these films. No crystalline phase was observed for nitrocalix[4]arene derivatives with longer or branched alkyl chains; this explains the limited NLO stability of films of these calixarenes. Scanning force microscopy on the aligned films of **9** showed two distinct surface lattice structures: a rectangular lattice ($a = 9.3$, $b = 11.7$ Å) and a pseudohexagonal lattice ($d \approx 11.4$ Å). The combination of these data with the interlayer distance of 8.9 Å (X-ray diffraction) allowed the packing of molecules of **9** in these structures to be fully elucidated at the molecular level.

Keywords: calixarenes · nonlinear optics · structure elucidation · supramolecular chemistry

Introduction

Materials with high second-order susceptibilities are important because of their possible applications in optical switching, frequency conversion, and data storage, etc.[1] For these nonlinear optical (NLO) applications, noncentrosymmetric crystals, such as urea, and inorganic materials, such as quartz and lithium niobate, are currently used.[2] Organic materials are of interest due to their good processability. Another reason for the current interest in organic NLO materials is the high hyperpolarizabilities of organic molecules that have electron-donating and -accepting groups connected by conjugated π-electron systems.

There are several possibilities for arranging nonlinear optically (NLO) active molecules to give materials with stable second-order nonlinear optical activity. The required stable noncentrosymmetric structure can be obtained by incorporation of the NLO-active molecules in solid solution films,[3] in stepwise-constructed multilayers,[4, 5] or in functionalized polymers.[6, 7] In these materials the degree of alignment of the NLO-active molecules is very important as the macroscopic NLO activity $\chi^{(2)}$ is directly related to the product of the molecular hyperpolarizability parameter β and the alignment factor $\langle \cos^3\theta \rangle$, where θ is the average angle of the molecules with the normal plane of the macroscopic film. A possible way to obtain aligned noncentrosymmetric structures is the controlled self-assembly of NLO-active molecules, for example by interaction of complementary groups. Such materials were reported by Marks et al.[4] and Katz et al.,[5] but these NLO-active multilayers are formed in a laborious layer-by-layer multistep procedure.

Earlier we reported that calix[4]arenes[8] with electron-donating propoxyl and electron-accepting nitro substituents exhibit promising micro- and macroscopic NLO properties.[9]

[*] Prof. Dr. Ir. D. N. Reinhoudt, Dr. P. J. A. Kenis, Ing. E. G. Kerver, Ing. B. H. M. Snellink-Ruël, Dr. J. F. J. Engbersen
Laboratory of Supramolecular Chemistry and Technology
Faculty of Chemical Technology, MESA Research Institute
University of Twente
P.O. Box 217, NL-7500 AE Enschede (The Netherlands)
Fax: (+31) 53-4892980
E-mail: smct@ct.utwente.nl

Dr. Ir. O. F. J. Noordman, Prof. Dr. N. F. van Hulst
Applied Optics Group, Faculty of Applied Physics, MESA Research Institute

Ing. G. J. van Hummel, Dr. S. Harkema
Chemical Physics Laboratory, Faculty of Chemical Technology, University of Twente

Dipl. Chem. H. Schönherr, Prof. Dr. G. J. Vancso
Polymer Materials Science and Technology,
Faculty of Chemical Technology, University of Twente

Dr. C. P. J. M. van der Vorst, Dr. J. Hare, Dr. S. J. Picken
Akzo Nobel Central Research, Department of Physical Chemistry

  0947-6539/98/0407-1225 $ 17.50+.25/0

Aligned films of these calix[4]arenes can be obtained by spin coating and subsequent electric-field poling. These materials have high nonresonance-enhanced frequency doubling coefficients which remain stable at room temperature for more than a year after an initial decay of 35–55%.[9] At high temperatures (>100 °C), however, most of the NLO activity in these films is lost.

Here we report the syntheses and properties of neat films of a number of tetranitrocalix[4]arene derivatives bearing different alkyl groups at the phenolic oxygen atoms. The main goal was to elucidate the origin of the unique high NLO stability of the films of tetranitrotetrapropoxycalix[4]arene by X-ray diffraction, angle-dependent second harmonic generation (SHG), and scanning force microscopy. Moreover, the conclusions of the experimental results are supported by solid-state molecular dynamics calculations.

Synthesis

The general route for the synthesis of a series of tetraalkoxytetranitrocalix[4]arenes **9**–**14** is depicted in Scheme 1. Tetra-*tert*-butylcalix[4]arene (**1**) was alkylated with various alkyl bromides in DMF at 60 °C with NaH as base to yield **2**–**5**. For calixarene **6** this one-step alkylation procedure was unsuccessful, and the four isobutyl groups were introduced by first

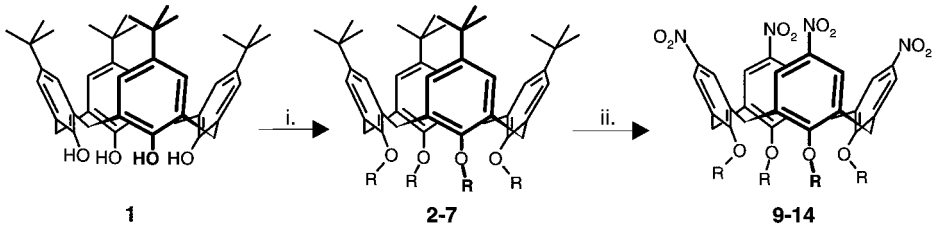

Scheme 1. Synthetic route to a series of tetranitrocalix[4]arene derivatives. i) NaH, RBr, DMF, 18 h, 60 °C. ii) TFA, 100% HNO_3, CH_2Cl_2, 5–20 min, room temperature. R = *n*-propyl (**2**, **9**); *n*-butyl (**3**, **10**); *n*-pentyl (**4**, **11**); *n*-hexyl (**5**, **12**); 2-methylpropyl (**6**, **13**); 3-methylbutyl (**7**, **14**).

O-alkylation of the distal 1- and 3-phenolic groups in CH_3CN with K_2CO_3 as base.[10] The resulting 1,3-diisobutoxycalix[4]-arene (**8**), was further alkylated in DMF with NaH as base to give **6**.[11] The four nitro groups of **9**–**14** were introduced in high yields by *ipso* nitration[12] in a mixture of 100% HNO_3 and trifluoroacetic acid (TFA) in dichloromethane.[13]

Optical Properties

Molecular optical properties: For a proper evaluation of the influence of alkyl substituents in the nitrocalix[4]arenes on the NLO properties in aligned thin films (vide infra), we first determined the effect of the different alkyl groups on the molecular optical properties. In solution the different alkyl groups do not significantly affect the electronic properties of **9**–**14** as shown by the nearly identical UV spectra with absorption maxima in the range of 290–292 nm. The data for the first hyperpolarizabilities[14] of the various tetranitrocalix[4]arene derivatives, as determined by hyper-Rayleigh scattering[42] (HRS), show that the influence of most alkyl substituents on this parameter is also small (Table 1). Only the calix[4]arene derivative with four bulky isobutoxyl groups **13** has a significantly higher hyperpolarizability ($\beta_{HRS} = (41 \pm 9) \times 10^{-30}$ esu). The steric requirements of the four isobutoxyl substituents force the four aromatic units of the calix[4]arene from the usual flattened (or pinched) cone conformation[15] into the more symmetrical cone conformation. The higher degree of alignment of the four π-donor/π-acceptor units of the calix[4]arene in the cone conformation corresponds to a higher β_{HRS} value.

Table 1. Measured absolute and normalized β_{HRS} values of tetranitrotetraalkoxycalix[4]arene derivatives **9**–**14**, angles of the π-donor-π-acceptor systems with respect to the molecular dipole axis as obtained by molecular modeling, and the calculated normalized β_{MM} values.

Compound	Experiment[a]		Molecular modeling		
	β_{HRS} [10^{-30} esu]	β_{HRS} (norm.)	angles [°][b]		β_{MM} (norm.)
9	31 ± 5	≡1	47.4	7.3	≡1
10	31 ± 7	0.96 ± 0.07	46.7	8.2	1.003
11	32 ± 8	1.02 ± 0.05	45.7	8.4	1.003
12	33 ± 6	1.10 ± 0.07	45.5	9.6	1.009
13	41 ± 9	1.24 ± 0.15	37.0	8.8	1.076
14	34 ± 8	1.03 ± 0.10	46.8	8.3	1.002

[a] Hyper-Rayleigh scattering (HRS, 1064 nm, Nd:YAG laser) in chloroform. [b] The angles in these two columns give the orientation of the two distal pairs of aryl groups with respect to the molecular dipole axis.

Molecular mechanics calculations of the structures of calixarenes **9**–**14** in the gas phase indeed show this effect of the isobutoxyl substituents on the orientation of the aromatic units.[16] Relative hyperpolarizabilities (β_{MM}) were calculated by adding the vectorial contributions of the four *p*-nitroalkoxyphenyl groups in the energy-minimized structures and subsequent scaling of the hyperpolarizability values to the value calculated for **9**.[17] The normalized β_{MM} value calculated (Table 1) for **13** is significantly larger than those of the other compounds.

Further experimental evidence[18] for the higher degree of alignment of the aryl rings in **13** was obtained from the single-crystal X-ray structure, which has orthorhombic symmetry (space group $P2_12_12_1$) and two calix[4]arene molecules in the asymmetric unit (Figure 1). The angles of the two distal pairs of aryl rings with respect to the molecular dipole axis of the two molecules are 53 and −13°, and 51 and −10°, respectively. These angles are significantly smaller than those of the propoxyl analogue **9** and indicate better alignment. In the crystal structure of **9** with one molecule of dichloromethane per calix[4]arene unit, the angles are 56 and −11°.[19] In an X-ray structure of crystals of solvent-free **9**, angles of 63 and −7° were found.[20]

0947-6539/98/0407-1226 $ 17.50+.50/0 *Chem. Eur. J.* **1998**, *4*, No. 7

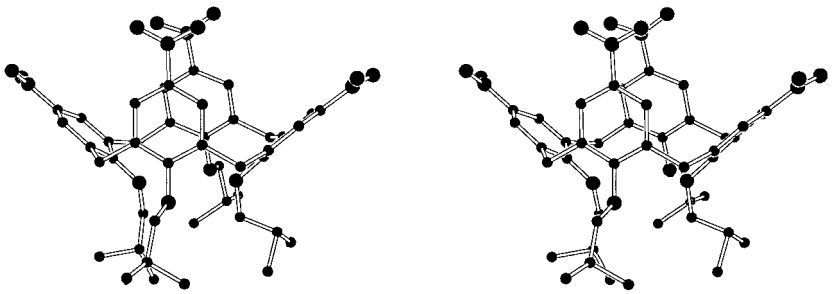

Figure 1. X-ray structure of **13** (stereoview).

Macroscopic nonlinear optical properties: Previously, we reported that films of neat **9** that were poled at 110 °C exhibit a fast initial relaxation of their NLO activity d_{33}.[9b] The d_{33} values measured directly after corona poling[21] with an electric field of about 10^8 V m^{-1} decreased by more than 35 or 85 % upon storage of the films at room temperature and 100 °C, respectively. After this fast initial decay, the residual NLO activity remained constant for a long period of time (Figure 2).

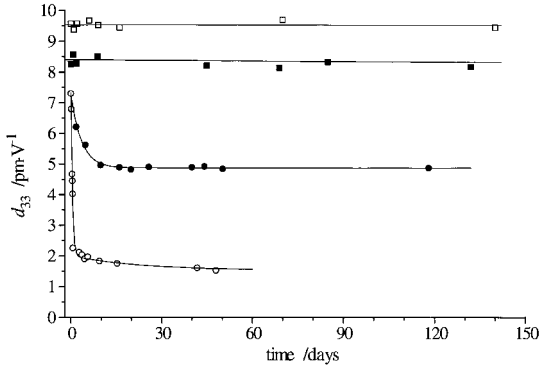

Figure 2. Stability of the NLO activity (d_{33} values at 1064 nm) of films **9** that were poled and stored at different temperatures. Circles (Kelderman et al.[9b]): poled at 110 °C. Squares (this work): poled at 150 °C. Solid symbols: stored at room temperature, open symbols at 80 °C.

Here we report the effects of different alkyl groups in the calix[4]arene and the influence of the poling conditions on the second-harmonic generation (d_{33})[22] properties of thin films of **9**–**14**. We have studied films of neat **9** poled at 150 °C in detail.

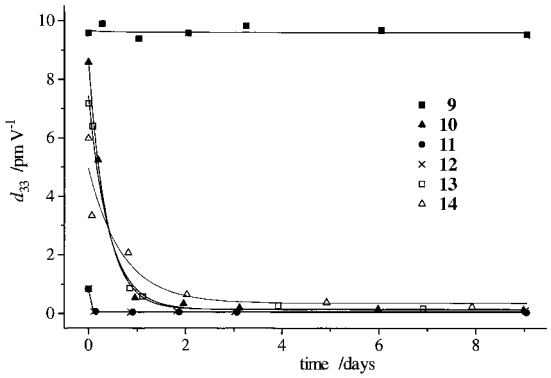

Figure 3. Time dependence of NLO activity (d_{33} values at 1064 nm) of films of **9**–**14** stored at 80 °C.

These films exhibit a high NLO activity (d_{33} value) that remains constant immediately after poling with an electric field of about 10^9 V m^{-1}. Most importantly, the d_{33} value of these films does not decay at room temperature or at 80 °C (Figure 2) over a period of more than one year. These properties are unique to films of **9**; in films of **10**–**14**, most of the NLO activity is lost within two days at 80 °C (Figure 3).

Morphology of Poled Films

The large difference in NLO stability of films of **9** compared to those of **10**–**14** (Figure 3) suggests that the molecular interactions in films of **9** must be distinctly different. This was investigated by optical microscopy, differential scanning calorimetry (DSC), and solid-state ^{13}C NMR spectroscopy.

Unpoled films of **9** which were heated at 110 °C for 15 min showed only a few birefringence spots under the polarizing microscope, which probably correspond to microcrystals that are formed during spin coating (Figure 4 top, left). After

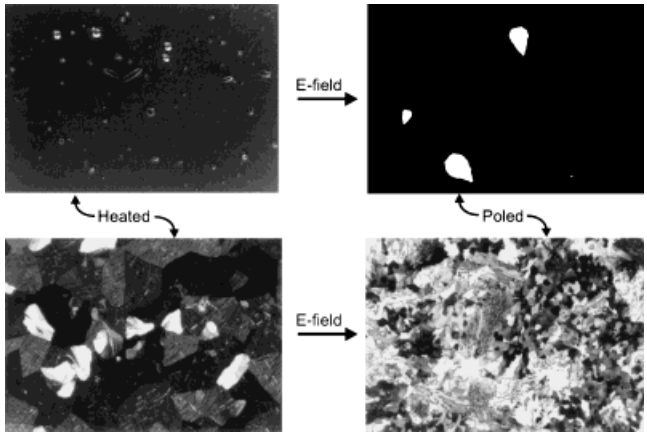

Figure 4. Polarization microscopy on films of **9** (160 × 110 μm). Top: Heated and poled at 110 °C; bottom: Heated and poled at 150 °C.

poling of the film at 110 °C, triangular, birefringent domains appear which are about 100 μm^2 in size (Figure 4 top, right).[23] An unpoled film that was heated at 150 °C for 15 min showed a structure completely covered by birefringent crystalline domains with sizes up to 1500 μm^2 (Figure 4 bottom, left).[24] After poling at 150 °C, these large domains disappear and are replaced by smaller birefringent domains (< 200 μm^2; Figure 4 bottom, right); clearly, recrystallization takes place in the electric field. The poled films of **10**–**14** show no birefringence; this indicates the presence of an amorphous phase. Such an amorphous molecular arrangement would explain the fast relaxation of the second-order NLO activity. Apparently, the phase transition between 110 and 150 °C takes place only in films of **9**.

For films of **9** which had been poled at 150 °C no change was observed in the birefringence pattern (Figure 4 bottom, right) on heating to 150 °C (10 K min^{-1}). However, in films poled at

110 °C the growth of several crystalline domains starts at 140 °C. Eventually, these films exhibited the same morphology as unpoled films that were heated at 150 °C for 15 min (Figure 4 bottom, left), and this structure remained unchanged after cooling to room temperature.

Differential scanning calorimetry (DSC) showed no enthalpy change for films of **9**[25] that were poled at 150 °C and for microcrystalline powders of **10**–**14**.[26] However, films of **9** that were poled at 110 °C exhibited an enthalpy change that is indicative of an irreversible endothermic phase transition between 130 and 140 °C, similar to that observed for unpoled films and microcrystalline samples of **9**.[24] In conclusion, the exceptional stability of films of **9** that were poled at 150 °C is due to a unique molecular packing, which is formed in a phase transition between 130–140 °C in an electric field.[24]

Optimization of optical properties of poled films: On poling films of **9**, the centrosymmetric, crystalline phase formed by heating to 150 °C recrystallizes to form a new, highly stable noncentrosymmetric phase consisting of much smaller birefringent domains (Figure 4 bottom). The presence of many domains, however, will lead to considerable light scattering when these films are used in optical waveguides. Therefore, the effect of the poling conditions on the extent of domain formation in films of **9** was investigated. Instead of slowly heating the film in 15 min to 150 °C and then applying the poling field (recrystallization), the film was heated to 150 °C within a few seconds in an electric field of 10^9 V m^{-1}.[27] In this way the phase transition from the amorphous phase to the crystalline phase (crystallization) takes place in an electric field. This has a dramatic effect on the size of the domains (Figure 5). Sharp-edged, birefringent domains with areas of up to 2.5×10^4 μm^2 are formed. The films with large and small domains exhibit the same NLO activity and stability. This was expected as our measurements of the second-harmonic generation were performed in the vertical direction. However, the lateral (non)linear optical properties of the film, which are important for applications, were improved, as the smaller number of domains dramatically decreases the amount of scattering.

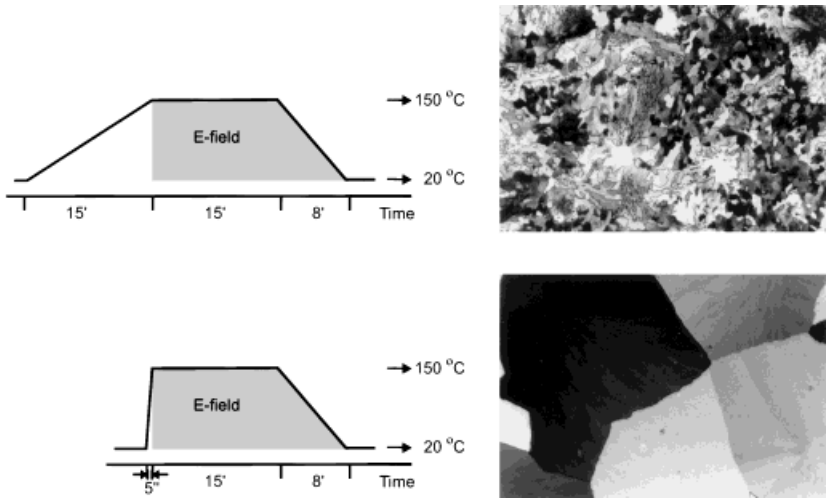

Figure 5. Effect of different poling conditions on the size of the domains formed in films of **9** (optical microscopy, crossed polarizers). Dimensions of micrographs: 160 × 110 μm.

Molecular Packing in Poled Films of 9

The packing of the molecules of **9** in the domains of films poled at 150 °C was investigated in order to explain the unusually high NLO stability. These investigations were performed on large-domain films by a combination of X-ray diffraction, surface second-harmonic generation, atomic force microscopy (AFM), and solid-state molecular dynamics calculations.

An interlayer lattice distance of 8.90 ± 0.05 Å was determined by X-ray diffraction on the films. The position of the reflection indicates that these layers are not parallel to the plane of the film.[28] Hence, the symmetry of an aligned film of **9** is lower than that of the unaligned film, which has an orthorhombic structure.[24]

The orientation of the molecules in a single domain of the poled film of **9** was investigated by measuring the second harmonic intensity as a function of the azimuthal angle of incidence of the beam ϕ.[29] The angle-dependent SHG pattern was measured for all four possible polarization combinations. By fitting these experimental data with theory, an orientation of the molecular dipole with respect to the normal of the film (b axis) of $13 \pm 2°$ ($\phi = 0°$) and $-13 \pm 2°$ ($\phi = 180°$) was determined.[29, 30] This indicates a zigzag or herringbone packing of the calix[4]arene molecules.

From the molecular and macroscopic NLO activities β_z and d_{33}, Equation (1) gives an alignment factor $\cos^3\theta$ of 0.85,

$$\langle \cos^3\theta \rangle = \frac{2\, d_{33}}{N F^3(\omega) \beta_z} \quad (1)$$

where θ is the angle of the molecular dipole with the normal vector of the film, N the number density of the molecules in the film, and $F(\omega)$ the local field factor.[31, 32] The high alignment factor of 0.85 determined by nonlinear optical measurements implies that the molecules of **9** are almost perfectly aligned in the film ($\theta = 15 \pm 3°$). This angle is in good agreement with those of $+13$ and $-13°$ found by angle-dependent second-harmonic generation. Such an alignment of the chromophores is considerably better than in most polymers. When **9** is covalently incorporated in poled polyimide films, $\cos^3\theta$ is 0.25 ($\theta = 51 \pm 3°$).[7] The alignment of the NLO-active moieties in these polyimide films is restricted by their limited mobility and because application of higher electric fields during poling leads to ablation of the film.[6a]

Atomic force microscopy was performed on single domains of aligned films of **9** to which the poling field was applied such that the positively polarized propoxyl groups pointed towards the outer surface. In the contact mode, molecular resolution was obtained for these films. The surface lattice constants of the rectangular structure **I** (Figure 6, left) and the pseudohexagonal structure **II** (Figure 6, right) are listed in Table 2. The symmetries of these lattices were de-

0947-6539/98/0407-1228 $ 17.50+.50/0 *Chem. Eur. J.* **1998**, *4*, No. 7

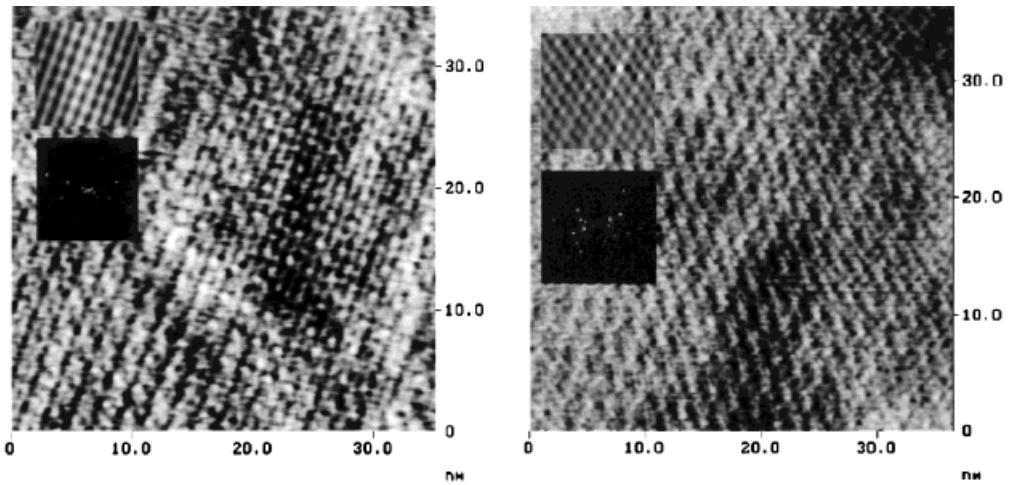

Figure 6. High-resolution AFM images of rectangular structure **I** (left), and pseudohexagonal structure **II** (right). Inserts: autocovariance images (top) and 2D Fourier spectra (bottom).

Table 2. Lattice constants a, b, and angle of registry from the structures found by AFM.

Symmetry	a [Å]	b [Å]	Angle [°]	Area per molecule [Å^2]
Rectangular **I**	9.3 ± 0.3	11.7 ± 0.3	90 ± 2	109
Hexagonal **II**	11.8 ± 0.3	10.9 ± 0.3	60 ± 2	114

duced from the autocovariance pattern of the images and from the pattern symmetry of the two-dimensional Fourier transfor of the images (inserts in Figure 6).

Films poled with electric fields of opposite sign have the highly polarizable nitro groups exposed to the surface instead of the propoxyl groups. Owing to the presence of these highly polar groups, the imaging force in contact-mode AFM (both in air and in water) is too high. As a result it was not possible to obtain images with lattice (molecular) resolution. The more hydrophilic character of these positively poled films compared to films that are poled with a negative electric field is evident from the large difference in the receding contact angles of water drops and from the large contact angle hysteresis (Table 3).[33]

The possible noncentrosymmetric packings of the molecules of **9** in the aligned films were calculated by solid-state molecular dynamics.[34] Figure 7 shows the (010) face (b face) and the (101) face of the monoclinic unit cell ($a = 10.94$, $b = 18.49$, $c = 10.67$ Å; $\alpha = \gamma = 90$, $\beta = 95.5°$) of one of the calculated structures. All structures exhibited the

Table 3. Results of contact angle measurements on films of **9** (water drop).

Sample	Contact Angle advancing ($\pm 3°$)	receding ($\pm 3°$)	Hysteresis[a] A–R [°]
Heated only	85	77	8
Positively poled[b]	83	45	38
Negatively poled[b]	88	75	13

[a] The hysteresis is the difference between advancing (A) and receding (R) contact angles. [b] Both films are poled using the same conditions (150 °C, optimized poling procedure resulting in large domains).

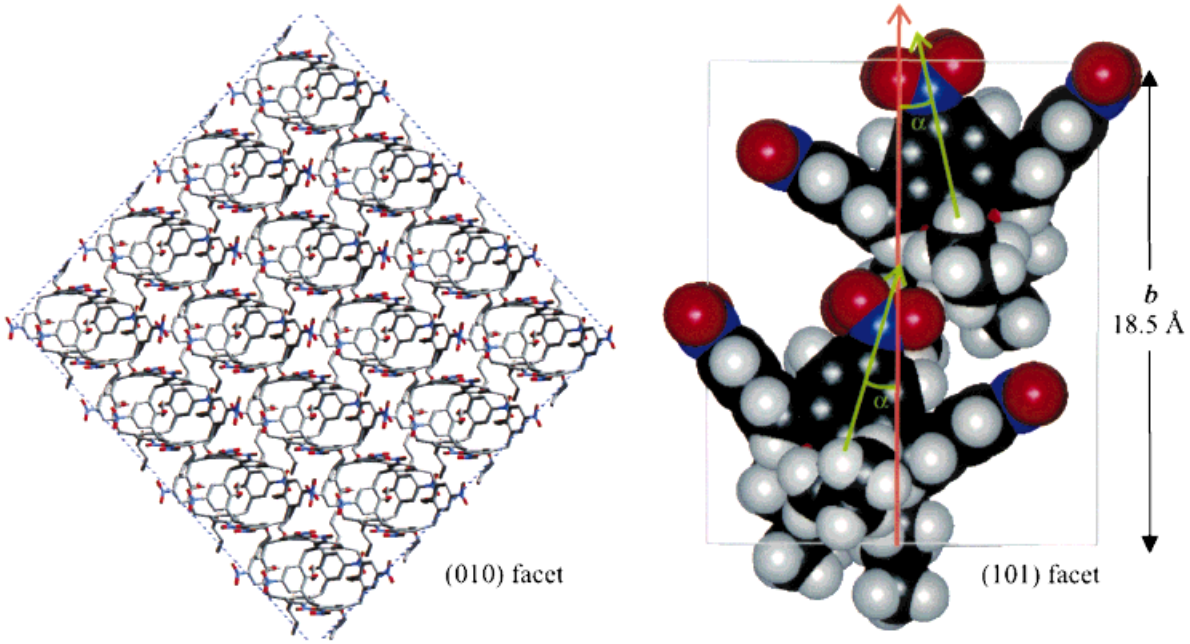

Figure 7. Calculated noncentrosymmetric packing of molecules of **9**. Left: (010) face (b face), 4×4 unit cells. Right: (101) face of a single unit cell.

typical zigzag stacking of the calixarenes. The major differences between the calculated structures lie in the orientation of the propyl groups. The calculated angles α of the molecular dipole axis of the molecules of **9** with respect to the *b* axis are $+14.7$ ($\phi = 0°$) and $-14.7°$ ($\phi = 180°$). These angles agree well with the values determined experimentally by angle-dependent SHG measurements ($13 \pm 2°$, vide supra).

The lattice parameters of the rectangular structure ($a =$ 10.9 Å, $b = 10.6$ Å) are also close to the parameters which were determined experimentally by AFM for the rectangular lattice **I** (Table 2). Moreover, the area per molecule in the (010) face of the calculated structure (116 Å^2) is close to that calculated for both the rectangular structure **I** (109 Å^2) and the pseudohexagonal structure **II** (114 Å^2, Table 2). Finally, the value of the calculated *b* axis (18.4 Å) is close to the interlayer distance found in the X-ray experiments on the aligned films (2×8.9 Å).

The area per molecule of the pseudohexagonal structure measured by AFM points to an orientation of the molecules as found in the rectangular packing. Translation of every second row of molecules in the calculated rectangular structure (Figure 7 left) over a distance of *a*/2 gives a pseudohexagonal lattice (Figure 8). The repeat distances of this lattice (10.9 and 12.0 Å) are well within the experimental

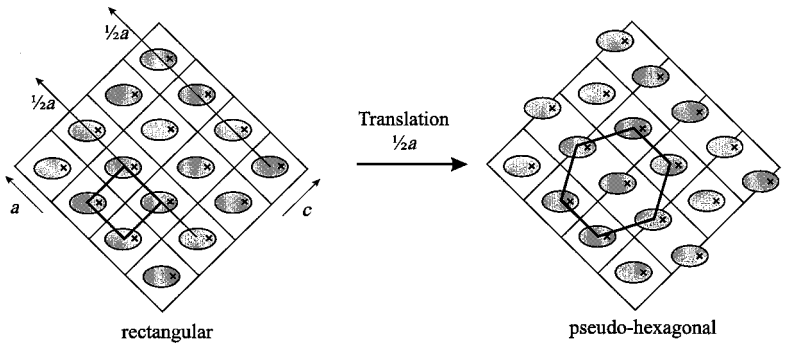

Figure 8. Schematic representation of a possible pseudohexagonal surface structure arising from the rectangular structure of the (010) face (Figure 7), as calculated by molecular dynamics. The crosses denote the nitro groups exposed at the surface, and ellipsoids represent the molecules of **9** (top view).

error of the values observed for pseudohexagonal structure **II** by AFM (Table 2). The coexistence of two different surface lattice structures can be explained by partial surface relaxation. A similar relaxation is also observed in unpoled films of **9**.[24]

The results obtained with the three experimental techniques, X-ray diffraction, angle-dependent SHG, and AFM, as well as the solid-state molecular dynamics calculations, are all consistent with a packing of the molecules of **9** in the aligned films in a manner similar to the structure shown in Figure 7. For this particular packing, the size and shape of the molecules of **9** result in favorable electrostatic interactions between the negatively polarized nitro groups of the calixarene molecules in one layer and the positively polarized phenoxyl groups of calixarene molecules in the neighboring layer ($d = 4.4 - 5.0$ Å). This arrangement can be clearly seen in the unit cell in Figure 7. This electrostatic lattice energy adds to the contributions of van der Waals forces and accounts for the unusually high stability of the noncentrosymmetric packing.

Conclusions

Stable thin films of tetranitrotetrapropoxycalix[4]arene (**9**) with a highly ordered molecular packing and second-order NLO properties were obtained by optimizing the poling conditions. The highly stable noncentrosymmetric structure of these films is achieved by a unique (re)crystallization process in an electric field at $130 - 140$ °C. The absence of such a metastable crystalline phase in nitrocalix[4]arene derivatives with longer or branched alkyl chains explains the lack of NLO stability in (amorphous) films of these compounds.

By a combination of X-ray diffraction, angle-dependent second-harmonic generation, and atomic force microscopy, and by comparing the experimental results with solid-state molecular dynamics calculations, the mode of packing of the molecules of **9** in the films was elucidated. Two surface lattice structures were observed by AFM and interpreted at the molecular level. The coexistence of rectangular and pseudohexagonal surface lattice structures is probably due to partial surface relaxation.

It can be concluded that the unprecedented high stability of the noncentrosymmetric packing in this supramolecular material is caused by attractive electrostatic interactions between the electronegatively polarized nitro groups of the molecules in one layer and the electropositively polarized propoxyl groups of the molecules in the adjacent layer.

Experimental Section

Synthesis: Melting points were determined with a Reichert melting point apparatus and are uncorrected. ^{1}H and ^{13}C NMR spectra were recorded on a Brucker AC 250 spectrometer in $CDCl_3$ (unless stated otherwise) at room temperature with residual solvent or Me_4Si as internal reference. Mass spectra were recorded with a Finnigan MAT 90 spectrometer with m-nitrobenzylalcohol (NBA) as matrix. Infrared spectra were recorded with a Jasco A-100 infrared spectrophotometer. Elemental analyses were carried out with a Carlo-Erbu Strumentazione model 1106 elemental analyzer. Hexane (petroleum ether, b.p. $60 - 80$ °C) and CH_2Cl_2 were freshly distilled from K_2CO_3. DMF was dried over molecular sieves (4 Å) for at least 3 d. NaH was used as a $55 - 65$ % dispersion in mineral oil and was washed three times with *n*-hexane prior to use. Other reagents were reagent grade and used without further purification. Flash column chromatography was performed on silica 60 (0.040 – 0.063 mm, 230 – 400 mesh) from E. Merck. All reactions were carried out under an argon atmosphere.

General procedure for 3 – 5 by alkylation of 1: To a well-stirred suspension of NaH (5 mmol) in DMF (20 mL) was added in small portions 5,11,17,23-tetra-*tert*-butylcalix[4]arene (**1**) (0.65 g, 1 mmol). After 1 h alkyl bromide (5 mmol) was added slowly. After the formation of foam ceased, the mixture was heated to 60 °C and stirred for 18 h. The reaction mixture was allowed to cool to room temperature and then poured into ice/water and filtered. The residue was dissolved in CH_2Cl_2 (50 mL) and washed with a saturated ammonium chloride solution (2×20 mL) and brine (2×20 mL). After drying over $MgSO_4$, the organic layer was concentrated in vacuo.

0947-6539/98/0407-1230 $ 17.50+.50/0 *Chem. Eur. J.* **1998**, *4*, No. 7

Trituration of the crude product with MeOH (if necessary) afforded the desired product in high purity. Tetrapropoxytetra-*tert*-butylcalix[4]arene (**2**) was synthesized according to a similar literature procedure.[9]

5,11,17,23-Tetra-*tert*-butyl-25,26,27,28-tetrabutoxycalix[4]arene (**3**) was obtained in 75% yield: m.p. 164–166 °C (CH_2Cl_2); ^{1}H NMR: $\delta = 6.78$ (s, 8H, ArH), 4.42, 3.11 (dd, $^2J_{AB} = 12.4$ Hz, 8H, $ArCH_2$), 3.86 (t, $^3J = 7.6$ Hz, 8H, OCH_2), 2.01 (quint, $J = 7.6$ Hz, 8H, $CH_2CH_2CH_3$), 1.46 (sext, $J = 7.7$ Hz, 8H, CH_2CH_3), 1.08 (s, 36H, $C(CH_3)_3$), 1.02 (t, $^3J = 7.3$ Hz, 12H, CH_3); ^{13}C NMR: $\delta = 153.77$ (ArCO), 144.12 (Ar*C*tBu), 133.85 ($ArCCH_2$), 124.86 (ArCH), 75.14 (OCH_2), 33.80 ($C(CH_3)_3$), 32.39 ($CH_2CH_2CH_3$), 31.47 ($C(CH_3)_3$), 31.06 (CH_2Ar), 19.39 (CH_2CH_3), 14.16 (CH_3); MS (FAB): *m*/*z* = 895.6 $[M+Na]^+$, calcd 895.7; analysis calcd for $C_{60}H_{88}O_4 \cdot 0.5\,H_2O$: C 81.67, H 10.17; found: C 81.88, H 10.28.

5,11,17,23-Tetra-*tert*-butyl-25,26,27,28-tetrapentoxycalix[4]arene (**4**) was obtained in 86% yield: m.p. 136–138 °C (CH_2Cl_2); ^{1}H NMR: $\delta = 6.77$ (s, 8H, ArH), 4.41, 3.10 (dd, $^2J_{AB} = 12.4$ Hz, 8H, $ArCH_2$), 3.85 (t, $^3J = 7.8$ Hz, 8H, OCH_2), 2.02 (quint, $J = 7.5$ Hz, 8H, OCH_2CH_2), 1.4 (m, 16H, CH_2CH_3, $CH_2CH_2CH_3$), 1.08 (s, 36H, $C(CH_3)_3$), 0.96 (t, $^3J = 6.7$ Hz, 12H, CH_3); ^{13}C NMR: $\delta = 153.78$ (ArCO), 144.12 (Ar*C*tBu), 133.87 ($ArCCH_2$), 124.86 (ArCH), 75.41 (OCH_2), 33.81 ($C(CH_3)_3$), 31.48 ($C(CH_3)_3$), 31.12 (CH_2Ar), 30.06 (OCH_2CH_2), 28.42 ($CH_2CH_2CH_3$), 22.92 (CH_2CH_3), 14.27 (CH_3); MS (FAB): *m*/*z*: 928.8 $[M^+]$, calcd 928.7; analysis calcd for $C_{64}H_{96}O_4 \cdot 0.5\,H_2O$: C 81.91, H 10.43; found: C 82.02, H 10.53.

5,11,17,23-Tetra(*tert*-butyl)-25,26,27,28-tetrahexoxycalix[4]arene (**5**) was obtained in 75% yield: m.p. 121–123 °C (CH_2Cl_2); ^{1}H NMR: $\delta = 6.77$ (s, 8H, ArH), 4.41, 3.11 (dd, $^2J_{AB} = 12.4$ Hz, 8H, $ArCH_2$), 3.84 (t, $^3J = 7.6$ Hz, 8H, OCH_2), 2.02 (m, 8H, OCH_2CH_2), 1.38 (br s, 24H, CH_2), 1.08 (s, 36H, $C(CH_3)_3$), 0.93 (t, $^3J = 6.6$ Hz, 12H, CH_3); ^{13}C NMR: $\delta = 153.84$ (ArCO), 144.15 (Ar*C*tBu), 133.87 ($ArCCH_2$), 124.85 (ArCH), 75.62 (OCH_2), 33.80 ($C(CH_3)_3$), 32.19 (OCH_2CH_2), 31.47 ($C(CH_3)_3$), 31.10 (CH_2Ar), 30.35, 25.97, 22.92 ($CH_2CH_2CH_2CH_3$), 14.13 (CH_3); MS (FAB) *m*/*z*: 1008.8 $[M+H]^+$, calcd 1007.8; analysis calcd for $C_{68}H_{104}O_4$: C 82.87, H 10.64; found: C 82.59, H 10.90.

5,11,17,23-Tetra-*tert*-butyl-25,27-diisobutoxy-26,28-dihydroxycalix[4]arene (**8**)[10] was obtained as a white powder in 57% yield: m.p. 270–272 °C (decomp) (CH_2Cl_2/hexane); ^{1}H NMR: $\delta = 7.81$ (s, 2H, OH), 7.04, 6.84 (2s, 8H, ArH), 4.29, 3.29 (dd, $^2J_{AB} = 12.9$ Hz, 8H, $ArCH_2$), 3.74 (d, $^2J = 6.1$ Hz, 8H, OCH_2), 2.33 (m, 4H, $CH(CH_3)_2$), 1.28, 0.99 (2s, 36H, $C(CH_3)_3$), 1.24 (d, $^2J = 6.7$ Hz, 24H, CH_3); ^{13}C NMR: $\delta = 151.02$, 149.74 (ArCO), 146.72, 141.18 (Ar*C*tBu), 132.71, 127.55 ($ArCCH_2$), 125.50, 125.03 (ArCH), 83.02 (OCH_2), 33.96, 33.80 ($C(CH_3)_3$), 31.73, 31.06 ($C(CH_3)_3$), 31.68 (CH_2Ar), 29.41 ($CH(CH_3)_2$), 19.51 (CH_3); MS (FAB): *m*/*z*: 761.1 $[M+H]^+$, calcd 761.5; analysis calcd for $C_{52}H_{72}O_4 \cdot 0.5\,H_2O$: C 81.10, H 9.55; found: C 80.76, H 9.70.

5,11,17,23-Tetra-*tert*-butyl-25,26,27,28-tetraisobutoxycalix[4]arene (**6**)[11] was obtained as a white powder by trituration with MeOH in 26% yield: m.p. > 310 °C (decomp) (MeOH); ^{1}H NMR: $\delta = 6.76$ (s, 8H, ArH), 4.51, 3.14 (dd, $^2J_{AB} = 12.4$ Hz, 8H, $ArCH_2$), 3.71 (d, $^2J = 6.5$ Hz, 8H, OCH_2), 2.24 (m, 4H, $CH(CH_3)_2$), 1.08 (s, 36H, $C(CH_3)_3$), 1.05 (d, $^2J = 6.7$ Hz, 24H, CH_3); ^{13}C NMR: $\delta = 154.08$ (ArCO), 143.66 (Ar*C*tBu), 133.04 ($ArCCH_2$), 125.08 (ArCH), 82.43 (OCH_2), 33.77 ($C(CH_3)_3$), 31.52 ($C(CH_3)_3$), 31.11 (CH_2Ar), 29.04 ($CH(CH_3)_2$), 20.35 (CH_3); MS (FAB): *m*/*z*: 873.1 $[M^+]$, calcd 872.7; analysis calcd for $C_{60}H_{88}O_4$: C 82.52, H 10.16; found: C 82.64, H 10.22.

5,11,17,23-Tetra-*tert*-butyl-25,26,27,28-tetraisopentoxycalix[4]arene (**7**) was obtained in 97% yield: m.p. 256–258 °C (CH_2Cl_2); ^{1}H NMR: $\delta = 6.77$ (s, 8H, ArH), 4.41, 3.12 (dd, $^2J_{AB} = 12.4$ Hz, 8H, $ArCH_2$), 3.91 (t, $^3J = 7.8$ Hz, 8H, OCH_2), 1.93 (quint, $J = 8$ Hz, 8H, OCH_2CH_2), 1.78 (m, 4H, $CH(CH_3)_2$), 1.08 (s, 36H, $C(CH_3)_3$), 0.98 (d, $^2J = 6.5$ Hz, 24H, CH_3); ^{13}C NMR: $\delta = 153.74$ (ArCO), 144.12 (Ar*C*tBu), 133.87 ($ArCCH_2$), 124.85 (ArCH), 73.91 (OCH_2), 39.00 (OCH_2CH_2), 33.80 ($C(CH_3)_3$), 31.47 ($C(CH_3)_3$), 31.16 (CH_2Ar), 25.57 ($CH(CH_3)_2$), 22.94 (CH_3); MS (FAB): *m*/*z* = 952.1 $[M+Na]^+$, calcd 951.7; analysis calcd for $C_{64}H_{96}O_4 \cdot 0.5\,H_2O$: C 81.91, H 10.42; found: C 82.14, H 10.59.

General procedure for the *ipso* nitration of 2–7 to give 9–14: To a solution of **2**–**7** (1 mmol) in CH_2Cl_2 (10 mL) was added trifluoroacetic acid (15 mmol). Subsequently, 100% nitric acid (20 mmol) was added in portions, and the mixture turned purple-black. After 5–20 min the reaction mixture was poured into ice/water, and CH_2Cl_2 (50 mL) was added. The aqueous layer was extracted with CH_2Cl_2 (2 × 50 mL), and the combined organic layers were washed with sodium bicarbonate solution (2 × 20 mL) and brine (2 × 20 mL), dried over $MgSO_4$, and concentrated under reduced pressure. Subsequently, the crude product was purified by column chromatography (CH_2Cl_2) or passed through a short (2 cm) silica filter (CH_2Cl_2) followed by recrystallization or trituration from CH_2Cl_2/MeOH. The yields of **10**–**12** and **14** were not optimized.

5,11,17,23-Tetranitro-25,26,27,28-tetra-*n*-propoxycalix[4]arene (**9**) was obtained in 98% yield. Spectroscopic data were as in ref. [12a].

5,11,17,23-Tetranitro-25,26,27,28-tetra-*n*-butoxycalix[4]arene (**10**) was obtained in 59% yield: m.p. 308–309 °C (CH_2Cl_2); ^{1}H NMR: $\delta = 7.56$ (s, 8H, ArH), 4.51, 3.39 (dd, $^2J_{AB} = 14$ Hz, 8H, $ArCH_2$), 3.99 (t, $^3J = 7.4$ Hz, 8H, OCH_2), 1.86 (quint, $J = 7.5$ Hz, 8H, $CH_2CH_2CH_3$), 1.44 (sext, $J = 7.5$ Hz, 8H, CH_2CH_3), 1.00 (t, $^3J = 7.3$ Hz, 12H, CH_3); ^{13}C NMR: $\delta = 161.70$ (ArCO), 142.86 ($ArCNO_2$), 135.45 ($ArCCH_2$), 124.00 (ArCH), 75.97 (OCH_2), 32.14 ($CH_2CH_2CH_3$), 31.11 (CH_2Ar), 19.15 (CH_2CH_3), 13.91 (CH_3); MS (FAB): *m*/*z*: 830.0 $[M+H]^+$, calcd 829.4; analysis calcd for $C_{44}H_{52}N_4O_{12}$: C 63.76, H 6.32, N 6.76; found: C 63.53, H 6.51, N 6.77.

5,11,17,23-Tetranitro-25,26,27,28-tetra-*n*-pentoxycalix[4]arene (**11**) was obtained in 63% yield: m.p. 244–246 °C (CH_2Cl_2); ^{1}H NMR: $\delta = 7.57$ (s, 8H, ArH), 4.50, 3.39 (dd, $^2J_{AB} = 14$ Hz, 8H, $ArCH_2$), 3.98 (t, $^3J = 7.4$ Hz, 8H, OCH_2), 1.87 (quint, $J = 7.5$ Hz, 8H, OCH_2CH_2), 1.38 (m, 16H, CH_2CH_3, $CH_2CH_2CH_3$), 0.95 (t, $^3J = 6.7$ Hz, 12H, CH_3); ^{13}C NMR: $\delta = 161.56$ (ArCO), 143.10 ($ArCNO_2$), 135.42 ($ArCCH_2$), 124.01 (ArCH), 76.21 (OCH_2), 31.19 (CH_2Ar), 29.83 (OCH_2CH_2), 29.08 ($CH_2CH_2CH_3$), 22.64 (CH_2CH_3), 14.03 (CH_3); MS (FAB): *m*/*z*: 885.2 $[M+H]^+$, calcd 885.4; analysis calcd for $C_{48}H_{60}N_4O_{12}$: C 65.14, H 6.83, N 6.33; found: C 65.02, H 7.05, N 6.30.

5,11,17,23-Tetranitro-25,26,27,28-tetra-*n*-hexoxycalix[4]arene (**12**) was obtained in 67% yield: m.p. 166–167 °C (CH_2Cl_2); ^{1}H NMR: $\delta = 7.57$ (s, 8H, ArH), 4.50, 3.39 (dd, $^2J_{AB} = 14$ Hz, 8H, $ArCH_2$), 3.97 (t, $^3J = 7.4$ Hz, 8H, OCH_2), 1.87 (m, 8H, OCH_2CH_2), 1.36 (br s, 24H, CH_2), 0.92 (t, $^3J = 6.5$ Hz, 12H, CH_3); ^{13}C NMR: $\delta = 161.66$ (ArCO), 142.90 ($ArCNO_2$), 135.43 ($ArCCH_2$), 124.01 (ArCH), 76.26 (OCH_2), 31.83 (OCH_2CH_2), 31.13 (CH_2Ar), 30.15, 25.69, 22.71 ($CH_2CH_2CH_2CH_3$), 13.98 (CH_3); MS (FAB): *m*/*z*: 941.6 $[M+H]^+$, calcd 941.9; analysis calcd for $C_{52}H_{68}N_4O_{12}$: C 66.36, H 7.28, N 5.95; found: C 66.02, H 7.52, N 5.91.

5,11,17,23-Tetranitro-25,26,27,28-tetraisobutoxycalix[4]arene (**13**) was obtained in 99% yield: m.p. > 310 °C (decomp) (CH_2Cl_2); ^{1}H NMR: $\delta = 7.55$ (s, 8H, ArH), 4.58, 3.44 (dd, $^2J_{AB} = 14.2$ Hz, 8H, $ArCH_2$), 3.85 (d, $^2J = 6.5$ Hz, 8H, OCH_2), 2.17 (m, 4H, $CH(CH_3)_2$), 1.03 (d, $^2J = 6.7$ Hz, 24H, CH_3); ^{13}C NMR: $\delta = 162.26$ (ArCO), 142.50 ($ArCNO_2$), 134.50 ($ArCCH_2$), 124.25 (ArCH), 82.70 (OCH_2), 31.27 (CH_2Ar), 29.38 ($CH(CH_3)_2$), 19.72 (CH_3); MS (FAB): *m*/*z*: 829.3 $[M+H]^+$, calcd 829.4; analysis calcd for $C_{44}H_{52}N_4O_{12}$: C 63.67, H 6.32, N 6.76; found: C 63.40, H 6.47, N 6.66.

5,11,17,23-Tetranitro-25,26,27,28-tetraisopentoxy-calix[4]arene (**14**) was obtained in 71% yield: m.p. 300–302 °C (CH_2Cl_2); ^{1}H NMR: $\delta = 7.57$ (s, 8H, ArH), 4.49, 3.40 (dd, $^2J_{AB} = 14.2$ Hz, 8H, $ArCH_2$), 4.03 (t, $^3J = 7.2$ Hz, 8H, OCH_2), 1.75 (m, 12H, OCH_2CH_2, $CH(CH_3)_2$), 0.97 (d, $^2J = 6.2$ Hz, 24H, CH_3); ^{13}C NMR: $\delta = 161.54$ (ArCO), 142.91 ($ArCNO_2$), 135.47 ($ArCCH_2$), 124.02 (ArCH), 74.68 (OCH_2), 38.73 (OCH_2CH_2), 31.14 (CH_2Ar), 25.28 ($CH(CH_3)_2$), 22.64 (CH_3); MS (FAB): *m*/*z*: 885.8 $[M+H]^+$, calcd 885.4; analysis calcd for $C_{48}H_{60}N_4O_{12}$: C 65.14, H 6.83, N 6.33; found: C 65.13, H 6.96, N 6.36.

X-ray diffraction: Single-crystal X-ray diffraction analysis of **13**: Data were collected on an Enraf-Nonius CAD4 diffractometer, $\omega - 2\theta$ scan mode, without absorption correction. The cell parameters were obtained from reorientation of matrices during measurement. Every 200 reflections 3 standard reflections were monitored. Crystal data: Orthorhombic, space group $P2_12_12_1$, $a = 19.461(2)$, $b = 21.074(2)$, $c = 21.368(2)$ Å, $V = 8763(1)$ Å^3, $Z = 8$, $\rho = 1.26$ g cm^{-3}, $\mu = 0.732$ cm^{-1}. Data collection: $Cu_{K\alpha}$ ($\lambda = 1.5418$ Å), $\theta/2\theta$ scan; $\theta = 2.5–60°$, 13359 measured reflections, 7111 independent reflections, 5897 observed reflections $[I > 3\sigma(I)]$, $T = 140$ K, $-21 < h < 21$, $0 < k < 23$, $0 < l < 23$, $R_{int} = 0.038$. The structure was solved by direct methods with SIR92[35] in the Enraf-Nonius software package[36] and were refined by full-matrix least-squares methods. Refinement was performed on $|F|$. Atomic scattering factors were taken from ref. [37]. The weighting scheme used was $w = 4F_o^2/\sigma^2(F_o^2)$ and $\sigma^2(F_o^2) = \sigma^2(I) + (pF_o^2)^2$ with $p = 0.04$. $R(F) = 0.087$, $wR(F) = 0.095$, $S = 4.0$, 801 parameters, $(\Delta/\sigma)_{max} = 0.77$, $\Delta\rho_{max} = 0.76$ e Å^{-3}. Yellowish prisms (0.4 × 0.3 × 0.2 mm) were obtained from dichloromethane/methanol by slow solvent evaporation.

The asymmetric unit consists of two molecules. All atoms were treated anisotropically. Hydrogen atoms were not included.[38]

X-ray diffraction on films: These measurements were performed on a Philips X-ray powder diffractometer with an X-ray beam from a cobalt source ($\lambda = 1.7903$ Å) incident on the film with an angle θ with respect to the plane of the film. The diffracted X-rays were measured at the same angle θ in reflection mode.

Film preparation, poling, and characterization: Poled films of **9**–**14** were prepared in a clean room with dust class 100 and 50% relative humidity. A solution of **9**–**14** in chloroform or cyclopentanone (5–10 wt%) was spun on Pyrex glass (2 s at 200 rpm, >40 s at 1000–2000 rpm) to give films with thicknesses in the range of 0.1–0.4 μm, as measured with a Sloan Dektak 3030 or Plasmos ellipsometer. These films were oriented at 110 or 150 °C for 15 min (unless stated otherwise) by corona poling[39] with a 25 μm tungsten wire at a distance of 10 mm, a corona voltage of 9 kV and a current of 10 μA. Films of tetranitrocalix[4]arene derivatives with melting points below the desired poling temperature were poled at 10 °C below the melting point. The films were allowed to cool to room temperature while the poling voltage was maintained. To determine the minimum electric field required for domain formation and to avoid surface ablation,[40] a corona poling setup equipped with a wire frame between nine corona needles and the hot stage was used (triode configuration).[41] Silicon wafers were used as substrate for the films since the Si surface can be regarded as the ground electrode. At a corona voltage of 12 kV and a wire-frame potential of 100 V some domains were formed; full coverage of the silicon surface was obtained at a wire-frame potential of 200 V. For films with a thickness of 0.2 μm, the required effective electric field was 0.5–1 kV μm^{-1}. The orientation parameters $\cos^3\theta$ of the films were calculated from Equation (1).[9, 31] The second-order susceptibility of the thin films was measured with a Maker-fringe setup at a fundamental wavelength of 1064 nm, with a Q-switched Nd:YAG laser and α-quartz as reference ($d_{11} = 0.51$ pm V^{-1}).[22] The hyper-Rayleigh scattering (HRS) measurements were performed with the same laser by the internal reference method[42] with a setup as described in refs. [29, 43]. Time-resolved measurements with a femtosecond laser show that the nitrocalix[4]arene derivatives do not exhibit multiphoton fluoresence.[44]

Surface second-harmonic generation: SHG measurements were performed with a Ti–sapphire laser (80 fs, 82 MHz, $\lambda = 900$ nm) positioned at an incident angle α. The reflected signal was detected with a photon-counting photomultiplier tube at the same angle α. The incident beam was focused on a single domain of the film, which was mounted on a rotating stage. The single domain and the focus of the incident beam were exactly aligned on the center of rotation. In this way the SHG signal of a single domain could be measured as a function of the azimuthal angle. Further details are given in refs. [29, 30].

Atomic force microscopy: AFM measurements were carried out with a NanoScope II and a NanoScope III multimode AFM (Digital Instruments (DI), Santa Barbara, CA, USA) in contact mode. The setup was equipped with a CCD camera that enabled the birefringent domains to be located prior to scanning. AFM scans were performed in air by using silicon nitride cantilevers (DI) with nominal spring constants of 0.38 N m^{-1} and 0.12 N m^{-1} (Si_3N_4, DI). The samples were attached to the sample holder disk with a cyanoacrylate adhesive. All images shown in this work correspond to plane-fitted raw data. For high-resolution imaging, the AFM setup was allowed to equilibrate for at least 24 h prior to measurements in air. Digital filtering was used to eliminate noise in additional images that were used to determine the lattice parameters (high-pass set to 4, low-pass set to 1). The lattice periodicities were observed both with and without the filters. The evaluation of the lattice constants and lattice symmetry has been described previously.[45] Cross-sectional plots of autocovariance patterns of the images were quantitatively evaluated to obtain the repeat length values. After correction for the sample height and recalibration of the instrument[46] the values of the repeat distances in corresponding directions of the observed lattices were averaged. Results are given as mean values including the standard deviation.

Molecular mechanics: The conformational energies of the structures of **9**–**14** were minimized in vacuum at 0 K by using Quanta/CHARMm 3.3[16] with ABNR (adopted basis set Newton–Raphson) until the root mean square (RMS) on the energy gradient was ≤ 0.01 kcal mol^{-1} Å^{-1}. Parameters were taken from Quanta 3.3. The molecules were charged to zero with a small excess of charge smoothed to nonpolar carbon and hydrogen atoms. No cutoff for the nonbonding interactions was applied, and a constant dielectric constant of $\varepsilon = 1$ was used.

Molecular dynamics: The simulations were carried out with the Discover program from Molecular Simulations Inc., San Diego, USA. The point charges of the starting geometry as taken from the single-crystal structure[19] were calculated for the entire calix[4]arene moiety by using the semiempirical molecular orbital program MOPAC.[47] The PM3 Hamiltonian was employed, and the resulting point charges were calculated with the ESP algorithm.[48] Electrostatic energies for the periodic boundary conditions were calculated by the Ewald summation technique.[49] The packing of dipole-aligned calix[4]arene molecules was achieved by the following method: Two molecules were graphically placed in either a stacked or a side-by-side noncentrosymmetric geometry. The orientation of the propyl groups was originally that of the centrosymmetric crystal structure. In an annealing simulation of energy minimization by molecular mechanics, 1 ps of molecular motion at 500 K by molecular dynamics, and reminimization were performed. The resulting energy and density of the annealed cell were compared to those of the original structure. For structures with higher total energy and higher density, the propyl groups were reoriented graphically so that they were placed symmetrically between the two molecules of the unit cell, and the annealing process was reapplied. Three structures with similar densities (1.22–1.25 g cm^{-3}) and energies were ultimately obtained by the cell-annealing process. The centrosymmetric single-crystal structure determined by X-ray diffraction has a density of 1.42 g cm^{-3} but contains four CH_2Cl_2 solvent molecules. A correction of the experimental cell volume and mass by the molecular volume and mass of four solvent molecules yields a density of 1.25 g cm^{-3}. After an initial temperature equilibration of the resulting cell at 298.4 K, a dynamics simulation was run for 30 ps at constant pressure, during which the cell dimensions were allowed to change.

Other instrumentation: Contact angles were measured with a computer-controlled Krüss G10 system, equipped with a CCD camera and video recorder. The reported angles are the averages of measurements on at least five drops of water.

DSC experiments were performed with a Perkin Elmer DSC7 calorimeter with heating rates of 20 or 30 °C min^{-1}.

Solid-state NMR experiments were carried out on a Varian Unity 400WB NMR spectrometer operating at 100 MHz for ^{13}C, equipped with a Jakobsen-design probehead in combination with a Sörensen heating unit and a Varian rotor speed control unit. The 5 mm diameter ZrO_2 spinners were spun at the magic angle speed of 4 KHz.

Polarization microscopy was performed on an Olympus BH2-UMA microscope equipped with an C35AD-4 camera.

Acknowledgements: We thank Ing. T. W. Stevens and Ing. A. M. Montanaro-Christenhusz of the Department of Chemical Analysis for recording the mass spectra and performing the elemental analyses. Dr. F. C. J. M. van Veggel is gratefully acknowledged for assistance with the molecular mechanics calculations. The authors thank H. Zhongxiu for her contribution to the HRS measurements and Dr. E. Klop for the powder X-ray diffraction analysis. Dr. H. Graafsma of the ESRF in Grenoble (France) is acknowledged for facilitating the X-ray measurements on the films. This research was supported by Akzo Nobel, Electronic Products, the OSF Micro Optics program of the University of Twente and the Netherlands Foundation for Chemical Research (SON) with support from the Netherlands Organization for Scientific Research (NWO).

Received: December 3, 1997 [F913]

[1] P. Prasad, D. J. Williams, *Introduction to Nonlinear Optical Effects in Molecules and Polymers*, Wiley, New York, **1991**.

[2] An alternative is the use of noncentrosymmetric crystals of organic NLO-active molecules, such as 2-methyl-4-nitroaniline (MNA): H. Itoh, K. Hotta, H. Takara, K. Sasaki, *Optics Commun.* **1986**, *59*, 299. Since less than 10% of all known crystal structures are noncentrosymmetric and crystal structures are difficult to predict on the basis of molecular structure, this strategy is not popular.

  0947-6539/98/0407-1232 $ 17.50+.50/0 *Chem. Eur. J.* **1998**, *4*, No. 7

[3] J. W. Wu, J. R. Valley, S. Ermer, E. S. Binkley, J. T. Kenney, G. F. Lipscomb, R. Lytel. *Appl. Phys. Lett.* **1991**, *58*, 225.

[4] a) D. Li, M. A. Ratner, T. J. Marks, C. Zhang, J. Yang, G. K. Wong, *J. Am. Chem. Soc.* **1990**, *112*, 7389; b) A. K. Kakkar, S. Yitzchaik, S. B. Roscoe, F. Kubota, D. S. Allen, T. J. Marks, W. Lin, G. K. Wong, *Langmuir* **1993**, *9*, 388.

[5] H. E. Katz, T. M. Sheller, M. Putvinski, M. L. Schilling, W. L. Wilson, C. E. Chidsey, *Science* **1991**, *254*, 1485.

[6] a) D. M. Burland, R. D. Miller, C. A. Walsh, *Chem. Rev.* **1994**, *94*, 31, and references therein; b) T. J. Marks, M. A. Ratner, *Angew. Chem.* **1995**, *107*, 167; *Angew. Chem. Int. Ed. Engl.* **1995**, *34*, 155, and references therein; c) E. T. Crumpler, J. L. Reznichenko, D. Li, T. J. Marks, W. Lin, P. M. Lundquist, G. K. Wong, *Chem. Mater.* **1995**, *7*, 596; d) D. Jungbauer, I. Terakoka, D. Y. Yoon, B. Reck, J. D. Swalen, R. Twieg, C. G. Wilsson, *J. Appl. Phys.* **1991**, *69*, 8011; e) S. Marturunkakul, J. I. Chen, R. J. Jeng, S. Sengupta, J. Kumar, S. K. Tripathy, *Chem. Mater.* **1993**, *5*, 743; f) G. H. Hsiue, J. K. Kuo, R. J. Jeng, J. I. Chen, X. L. Jiang, S. Marturunkakul, J. Kumar, S. K. Tripathy, *ibid.* **1994**, *6*, 884; g) Z. Liang, L. R. Dalton, S. M. Garner, S. Kalluri, A. Chen, W. H. Steier, *Chem. Mater.* **1995**, *7*, 941; h) D. Yu, A. Gharavi, L. Yu, *Macromolecules* **1995**, *28*, 784; i) *J. Am. Chem. Soc.* **1995**, *117*, 11680–11686; j) T. Verbiest, D. M. Burland, M. C. Jurich, V. Y. Lee, R. D. Miller, W. Volksen, *Science* **1995**, *268*, 1604; k) R. Hagen, O. Zobel, O. Sahr, M. Biber, M. Eckl, P. Strohriegl, C. D. Eisenbach, D. Haarer, *J. Appl. Phys.* **1996**, *80*, 3162–3166.

[7] P. J. A. Kenis, O. F. J. Noordman, N. F. van Hulst, J. F. J. Engbersen, D. N. Reinhoudt, B. H. M. Hams, C. P. J. M. van der Vorst, *Chem. Mater.* **1997**, *9*, 596–601.

[8] For reasons of clarity and to save space, the name calix[4]arene was used instead of the IUPAC name pentacyclo[19.3.1.$3^{,7}1^{8,13}1^{15,19}$]-octacosa-1(25),3,5,7(28),9,11,13(27),15,17,18(26),31,23-dodecane.

[9] a) E. Kelderman, G. J. T. Heesink, L. Derhaeg, T. Verbiest, P. T. A. Klaase, W. Verboom, J. F. J. Engbersen, N. F. van Hulst, A. Persoons, D. N. Reinhoudt, *Angew. Chem.* **1992**, 104, 1107; *Angew. Chem. Int. Ed. Engl.* **1992**, *31*, 1075; b) E. Kelderman, L. Derhaeg, G. J. T. Heesink, W. Verboom, J. F. J. Engbersen, N. F. van Hulst, K. Clays, A. Persoons, D. N. Reinhoudt, *Adv. Mater.* **1993**, *5*, 925.

[10] According to the synthesis of 25,27-dipropoxy-calix[4]arene as described in: R. H. Vreekamp, W. Verboom, D. N. Reinhoudt, *Recl. Trav. Chim. Pays-Bas* **1996**, *115*, 363-370.

[11] According to the synthesis of 5,11,17,23-tetra(*tert*-butyl)-25,27-dipropoxy-26,28-bis(3-phthalimidopropoxy) calix[4]arene as described in ref. [7].

[12] a) W. Verboom, A. Durie, R. J. M. Egberink, Z. Asfari, D. N. Reinhoudt, *J. Org. Chem.* **1992** *57*, 1313; b) A. Casnati, L. Domiano, A. Pochini, R. Ungaro, M. Carramolino, J. Oriol Magrans, P. M. Nieto, J. López-Prados, P. Prados, J. de Mendoza, R. G. Janssen, W. Verboom, D. N. Reinhoudt, *Tetrahedron* **1995**, *51*, 12699-12720.

[13] The use of TFA results in shorter reaction times, less decomposition, shorter purification procedures and higher yields than the procedures described earlier using glacial acetic acid[12a] or 65% HNO_3 and H_2SO_4[12b]. For example, **9** is now obtained in quantitative yield as opposed to 67% in the procedure described in ref. [12a].

[14] The conventional definition of the hyperpolarizability, as described in R. Bersohn, Y-H. Pao, H. L. Frisch, *J. Chem. Phys.* **1966**, *45*, 3184 or ref. [1], was used here.

[15] Also called pinched cone conformation: J. Scheerder, R. H. Vreekamp, J. F. J. Engbersen, W. Verboom, J. P. M. Van Duynhoven, D. N. Reinhoudt, *J. Org. Chem.* **1996**, *39*, 720–728.

[16] The Quanta/CHARMm program (MSI, Burlington, MA, USA), and the CHARMM force field are described in: a) B. R. Brooks, R. E. Bruccoleri, B. D. Olafsen, D. J. States, S. Swaminathan, M. Karplus, *J. Comput. Chem.* **1983**, *4*, 187; b) F. A. Momany, V. J. Klimkowski, L. Schäfer, *J. Comput. Chem.* **1990**, *11*, 654; c) F. A. Momany, R. Rone, H. Kunz, R. F. Frey, S. Q. Newton, L. Schäfer, *J. Mol. Structure* **1993**, *286*, 1.

[17] Four independent β_{333} vectors connecting the oxygen atom of the propoxyl group and the nitrogen atom of the nitro group of each chromophoric unit were calculated. These β_{333} vectors were added in a vectorially way to give the β_{333} of the calix[4]arene structure.

[18] Additionally, a shift of 0.1 ppm to lower field of the dd system of the methylene units that connect the phenol moieties was observed for the 2-methylpropylcalix[4]arene derivatives **6** and **13**. This can be explained by the inward bending of the aryl rings (deshielding).

[19] E. Kelderman, L. Derhaeg, W. Verboom, J. F. J. Engbersen, S. Harkema, A. Persoons, D. N. Reinhoudt, *Supramol. Chem.* **1993**, *2*, 183–190.

[20] P. J. A. Kenis, J. F. J. Engbersen, D. N. Reinhoudt, S. Houbrechts, K. Clays, A. Persoons, O. F. J. Noordman, N. F. van Hulst, G. J. van-Hummel, S. Harkema, unpublished results.

[21] a) E. G. J. Staring, *Recl. Trav. Chim. Pays-Bas* **1991**, *110*, 492; b) E. G. J. Staring, *Adv. Mater.* **1991**, *3*, 401.

[22] The Maker fringe patterns were analyzed as described in J. Jerphagon, S. K Kuntz, *J. Appl. Phys.* **1970**, *41*, 1667–1681.

[23] These domains probably represent the parts of the films which have a stable NLO activity, whereas the nonbirefringent area may represent the domains for which the NLO activity decays within a few days (Figure 2).

[24] The typical phase behavior of **9**, as well as the surface properties and the molecular packing of unpoled films of **9** as studied by scanning force microscopy are described in H. Schönherr, P. J. A. Kenis, J. F. J. Engbersen, A. J. R. L. Hulst, S. Harkema, D. N. Reinhoudt, G. J. Vancso, *Langmuir*, in press.

[25] These samples are prepared by scraping the poled material from the glass substrate with a scalpel.

[26] For the powders of **10**–**14**, the absence of a phase transition was confirmed by solid-state ^{13}C NMR spectroscopy. The narrow line widths and the thermally induced sharpening of the different resonances of powdered samples of **10**–**14** indicate the polycrystalline character of these compounds. Only **10** exhibits a minor irreversible phase transition in the solid-state NMR spectrum between 100 and 150 °C, which could, however, not be detected by DSC. Unfortunately, it was not possible to obtain ^{13}C NMR spectra from poled or unpoled films of **9** with an acceptable signal-to-noise ratio. To obtain sufficient material for NMR analysis (15 mg), it would be necessary to align over 600 films.

[27] Whereas such high fields of 10^9 V m^{-1} can be used for these crystalline films without damaging the structure, most polymer films suffer severe ablation damage at electric fields of $>10^8$ V m^{-1}.

[28] To determine the angle between the plane of the film and the crystal plane, angle-dependent X-ray measurements would be necessary (rotation of film). If the angle were also about 15° (like the molecular orientation with respect to the normal of film), a *c* axis of 8.6 Å can be calculated. Unfortunately, both the poled and unpoled films of **9** were too thin to determine the structure in more detail by X-ray crystallography.

[29] These experiments are described in full detail in O. F. J. Noordman, *Second Harmonic Generation using Organic Materials*, Ph. D. Thesis, University of Twente, Enschede, The Netherlands, **1996**.

[30] N. F. van Hulst, O. F. J. Noordman, P. J. A. Kenis, H. Schönherr, R. Veeneman, J. F. J. Engbersen, G. J. Vancso, D. N. Reinhoudt, unpublished results.

[31] C. P. J. M. van der Vorst, S. J. Picken, *J. Opt. Soc. Am. B* **1990**, *7*, 320–325.

[32] For the number density *N* a value of 10^{27} m^{-3} was used, as obtained from the single-crystal X-ray structure.[19] The local field factor ($F = 3.2$) was determined from refractive index measurements ($n = 1.57$) on films of **9**, as described in ref. [29].

[33] J. Drelich, W.-H. Jang, J. D. Miller, *Langmuir* **1997**, *13*, 1345–1351.

[34] To reduce the volume of the calculations, only two calix[4]arene molecules were placed in the unit cell. Initially, they were placed either in a stacked or in a side-by-side way, but after the annealing procedure (see Experimental Section) both resulted in a similar unit cell as applied in the actual MD run.

[35] M. C. Burla, M. Camalli, G. Cascarano, C. Giacovazzo, G. Polidori, R. Spagna, D. Viterbo, *SIR. J. Appl. Cryst.* **1989**, *22*, 389-393.

[36] a) C. K. Fair, Molen, an Interactive Intelligent System for Crystal Structure Analysis, , Enraf-Nonius, Delft, The Netherlands, **1990**; b) CAD4 Operations Manual, Enraf-Nonius, Delft, The Netherlands, **1977**.

[37] *International Tables for Crystallography*, *Vol. C*, **1992**, Tables 4.2.6.8, 6.1.1.4.

[38] Crystallographic data (excluding structure factors) for the structure reported in this paper have been deposited with the Cambridge

Crystallographic Data Centre as supplementary publication no. CCDC-100844. Copies of the data can be obtained free of charge on application to CCDC, 12 Union Road, Cambridge CB2 1EZ, UK (fax: (+44) 1223-336-033; e-mail: deposit@ccdc.cam.ac.uk).

[39] a) R. B. Comizzoli, *J. Electrochem. Soc. Solid-State Sci. Techn.* **1987**, 424; b) M. A. Mortazavi, A. Knoesen, S. T. Kowel, B. G. Higgens, A. Dienes, *J. Opt. Soc. Am. B* **1989**, *6*, 733.

[40] For films of **9**, surface ablation was observed in the corona set-up without the wire-frame when thin (0.10 mm) glass substrates were used. This was only occasionally observed on thick (1.00 mm) glass substrates.

[41] R. G. Vyverberg in *Xerography and Related Processes*, (Eds.: J. H. Dessauer, H. E. Clark), The Focal Press, London, **1984**.

[42] K. Clays, A. Persoons, *Phys. Rev. Lett.* **1991**, *66*, 2980.

[43] G. J. T. Heesink, A. G. T. Ruiter, N. F. Van Hulst, B. Bölger, *Phys. Rev. Lett.* **1993**, *71*, 999 – 1002.

[44] P. J. A. Kenis, O. F. J. Noordman, S. Houbrechts, G. J. van Hummel, S. Harkema, F. C. J. M. van Veggel, K. Clays, J. F. J. Engbersen, A. Persoons, D. N. Reinhoudt, unpublished results.

[45] H. Schönherr, G. J. Vancso, B.-H. Huisman, F. C. J. M. van Veggel, D. N. Reinhoudt, *Langmuir* **1997**, *13*, 1567.

[46] a) D. Snétivy, G. J. Vancso, *Langmuir* **1993**, *9*, 2253; b) M. Jaschke, H. Schönherr, H. Wolf, H.-J. Butt, E. Bamberg, M. K. Besocke, H. Ringsdorf, *J. Phys. Chem*. **1996**, *100*, 2290.

[47] J. J. P. Stewart, *QCPE* **1986**, *18*, 455.

[48] a) F. Momany, *J. Chem. Phys.* **1978**, *82*, 592; b) S. R. Cox, D. E. Williams, *J. Comput. Chem.* **1981**, *2*, 304.

[49] M. P. Allen, D. J. Tildesley, *Computer Simulation of Liquids*, Oxford University Press, Oxford, **1987**, p. 156.

0947-6539/98/0407-1234 $ 17.50+.50/0